Flow measurements during RivGen deployment Igiugig, AK – Summer 2014

Jim Thomson, Levi Kilcher, and Brian Polagye

revision: November 12, 2014

Abstract

Velocity measurements during the Ocean Renewable Power Company's 'RivGen' Turbine deployment at Igiugig, AK, are used to assess the variability of the river flow. The first objective is to understand the spatial variability of the inflow velocities for RivGen, in particular the strong spanwise shear that occurs at the RivGen location. The second objective is to understand the time variability of inflow velocities, in particular the streamwise coherence of the inflow velocities. Results suggest that the river flow is approximately steady, in the mean sense, at any particular location in the river, with random turbulent fluctuations that are around 10% of the mean flow. The mean flow in the center channel of the river is 2.5 m/s, with reductions near the riverbanks and in the shallows. As the flow is quasi-steady, the data from various stations can be gridded to a synoptic flow map around the turbine. A cross-section of this flow map immediately upstream of the turbine shows strong inflow velocity gradients across the turbine. Spectral analysis and lagged correlation results indicate that temporal fluctuations at a given point are dominated by large scale fluctuations (> 10 s), such that measurements at the turbine location are just as useful for inflow control implementation as upstream measurements.

1 Site description

The ORPC deployment site on the Kvichak River is just downstream of the village of Igiugig, AK. A local coordinate system is defined in Figure 1, with $+x$ downstream (u component of velocity), $+y$ cross-river towards the village (v component of velocity), and $+z$ upwards (w component of velocity). The origin is at the nominal center of the turbine (59.324745° N, 155.915092° deg W) and the rotation from an east-north-up (true) coordinate system is 107° deg clockwise.

The river is approximately 5 m deep and 150 m wide at the deployment site, and the turbine hub-height is approximately 2 m below the surface. The turbine is 1.5 m in diameter. The flow is maximum $u \approx 2.5$ m/s in the center of the river.

2 Data collection & Analysis

Inflow velocities were measured upstream of the RivGen turbine in Iguigig, AK, from Aug 15 to 25, 2014. Measurements were made with six Nortek Aquadopp profilers deployed in a down-looking orientation from surface catamaran platforms (Doppcats, see Figure 2). The platforms were towed

Figure 1: RivGen deployment location and local coordinate system at Igiugig, AK.

Figure 2: Doppcat platform for down looking Nortek Aquadopp velocity profiler (left) and sounding weight platform for Nortek Vector velocimeter (right) at Igiugig, AK.

on tethers at 10 m spacing astern of small skiffs, which held station and sampled at 1 Hz for 10 minutes at a variety of locations upstream of the turbine. The station-holding approach was adopted when the anchors for the Doppcats did not hold sufficiently in the strong river flows and cobbled riverbed. Locations were recorded at 5 Hz using Qstarz BT-Q1000 receivers, and this information was merged with the velocity measurements in post-processing.[1]

Two additional measurements were made. First, a Nortek Vector velocimeter was deployed on a "turbulence torpedo lowered from a davit at the stern of the skiff to provide high-fidelity turbulence measurements at 16 Hz. Second, a Nortek Signature profiler (a new 5-beam instrument) was deployed down-looking on a Doppcat and released to freely drift over the turbine and observed flow patterns at 8 Hz. The data return was 100% from all instruments, and the resulting cumulative sampling time (sum of all instruments) is about 300 hours of river velocity data.

The velocity measurements, which vary in space and time, are subject to measurement uncertainties which are predominantly the Doppler noise Δu_n of the instruments. The streamwise flow u, for example, is decomposed as

$$u(x,y,z,t) = \bar{u}(x,y,z) + u'(x,y,z,t) \pm \Delta u_n \pm \Delta u_{sk}, \tag{1}$$

where $\bar{u}$ is the mean flow calculated from 10 minutes of data and Δu_n is estimated as a constant

[1]Merging the GPS and Aquadopp measurements would typically include a 16 second offset between GPS timestamps and the Network Time Protocol (NTP). However, the PC used to deploy and sync the Aquadopps was set directly to the GPS time, daily, using a handheld unit in the field.

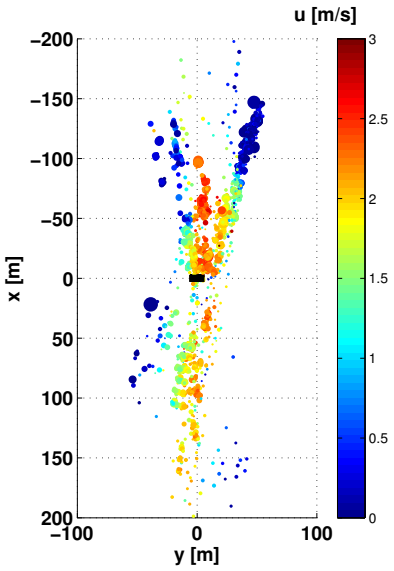

Figure 3: All mean streamwise flow results from the Doppcat station keeping measurements. Points are colored by flow speed and sized by number of observations. The turbine location is shown by a thick black line at the origin.

noise level of 0.04 m/s for the 2 MHz aquadopps and 0.01s m/s for the 1 MHz aquadopps. There are additional uncertainties resulting from imperfect station keeping, measured via GPS as $\Delta u_{sk} \approx 0.1$ m/s.

The space and time variables also have uncertainties,

$$x = x \pm \Delta x_{gps} \pm \Delta x_{bs} \pm \Delta x_{sk}, \qquad t = t \pm \Delta t_{cd}, \tag{2}$$

which are the result of GPS errors ($\Delta x_{gps} \approx 5$ m), beam spreading of the down looking Aquadopps ($\Delta x_{bs} \approx 3$ m), imperfect station keeping ($\Delta x_{sk} \approx 5$ m), and clock drift ($\Delta t \approx 1$ s).

These uncertainties are assumed to be uncorrelated, and averaging of results significantly reduces the uncertainty, such that robust estimates of the mean flow $\bar{u}(x, y, z)$ at a given position are repeatable. However, spatial gradients of the mean flow will be smoothed over scales finer than the uncertainties Δx. Beyond the mean estimates, robust estimates of the turbulence intensity TI are possible if the additional sources of variance from uncertainties are removed following *Thomson et al.* (2012),

$$TI(x, y, z) = \frac{\sqrt{\langle u'(x, y, z, t)^2 \rangle - \Delta u_n^2 - \Delta u_{sk}^2}}{\bar{u}(x, y, z)}, \tag{3}$$

where $\langle u'(x, y, z, t)^2 \rangle$ indicates an ensemble value over 10 minutes of observations at a particular (x, y) station.

3 Results

The river velocity measurements show robust spatial pattern in the mean streamwise flow $\bar{u}(x, y, z)$, with random turbulent fluctuations in time that are approximately $TI \approx 10\%$ of the mean flow at

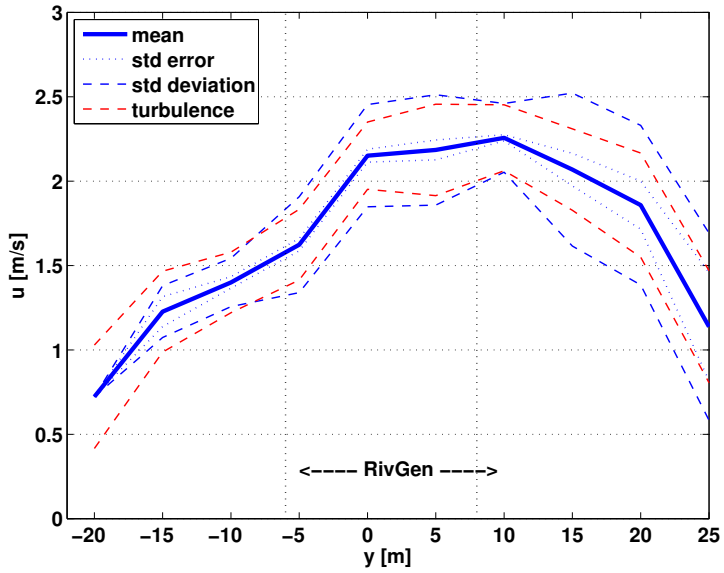

Figure 4: Lateral shear shown as the streamwise flow u versus cross-river dimension y. Results are the average from 338 stations lasting at least 10 minutes each, collected at positions immediately upstream of the turbine ($-20 < x < 0$ m). The blue dotted line is the standard error in determining the mean flow at each y. The blue dashed line is the standard deviation of individual stations. The red dashed line is variation expected from the measured turbulence intensity. The RivGen turbine cross-section is shown as a black line ($-6 < y < 8$) m.

any given location. Figure 3 shows all the $\bar{u}$ observations collected with the Doppcats over 10 days. The temporal and spatial variations are separated by binning individual 10-minute ensembles into 5-m resolution grid cells (using the local coordinate system) and assessing sensitivity. The spatial variations in the mean flow are extreme, and in many cases the uncertainty in position Δx is a greater source of velocity changes than the $TI \approx 10\%$ turbulence intensity at any given point.

In the following subsections, the spatial patterns are addressed are: cross-river y (i.e., lateral shear of inflow velocities), depth profiles z (i.e., vertical shear of inflow velocities), and streamwise x (i.e., inflow turbulence and wake deficit). For each axis investigated, the robustness of the spatial pattern is quantified with the standard error and standard deviation of the gridded mean velocity result and this is compared with velocity fluctuations expected from the average turbulence intensity TI in each grid cell.

In a final subsection, temporal variability is examined using frequency spectral and coherence metrics.

3.1 Lateral shear

The lateral shear of inflow velocities across the turbine (i.e., from port to starboard) is the most striking spatial pattern. As shown in Figure 4, the mean inflow velocity varies from 1.6 m/s at the port side of the turbine ($y = -6$ m) to 2.3 m/s at the starboard side of the turbine ($y = 8$ m). This 44% increase in speed is a 200% increase in the power density of the flow and likely has profound impacts on the performance of the turbine. This mean flow pattern is robust, as shown by the standard error lines in Figure 4. However the individual ensembles have significant

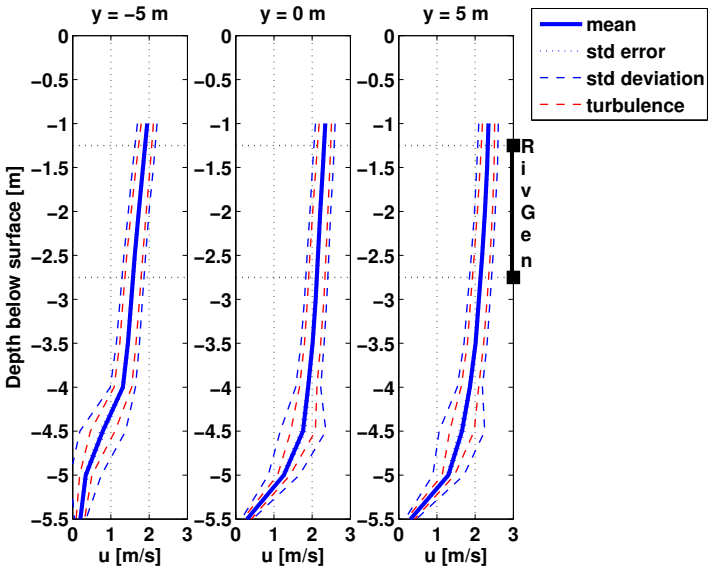

Figure 5: Vertical shear shown as the streamwise flow u versus depth below the surface at three positions in the cross-river direction: nominally turbine port ($y = -5$ m), turbine center ($y = 0$ m) and turbine starboard ($y = +5$ m). Results are the average from 338 stations lasting at least 10 minutes each, collected at positions immediately upstream of the turbine ($-20 < x < 0$ m). The blue dotted line is the standard error in determining the mean flow at each y. The blue dashed line is the standard deviation of individual stations. The red dashed line is variation expected from the measured turbulence intensity. The RivGen rotor sweep is shown as a black line ($-2.75 < z < -1.25$) m.

scatter, as by the standard deviation lines in Figure 4. In fact, the standard deviations obtained from the uncertainties in spatial binning are similar, and generally exceed, the velocity fluctuations attributed to turbulence within each ensemble.

The observed shear is expected given the proximity to a river bend and the ADCP surveys complete the previous year by Terrasonde. It appears that deployment of the RivGen turbine a few meters farther east, at approximately $0 < y < 12$ m, would have provided a much more uniform inflow condition. Although a few meters may seem an extreme sensitivity in a river that is 150 m wide, the deep region near the river bend is a much smaller feature and clearly controls the flow.

3.2 Vertical shear

There is minimal vertical shear in the streamwise inflow velocities upstream of the turbine. As shown in Figure 5, RivGen is sufficiently far above the riverbed and sufficiently small in diameter relative to the river depth that vertical variations are typically less than 10% of the mean flow value at hub height $z = -2$ m below the surface. Vertical shear is assessed at three locations in cross-river dimension y, nominally turbine port ($y = -5$ m), turbine center ($y = 0$ m) and turbine starboard ($y = +5$ m). The pattern from these three profiles is consistent with the lateral shear result, in which flow is strongest at the starboard side of the turbine and in which spatial uncertainties of exceed turbulent fluctuations.

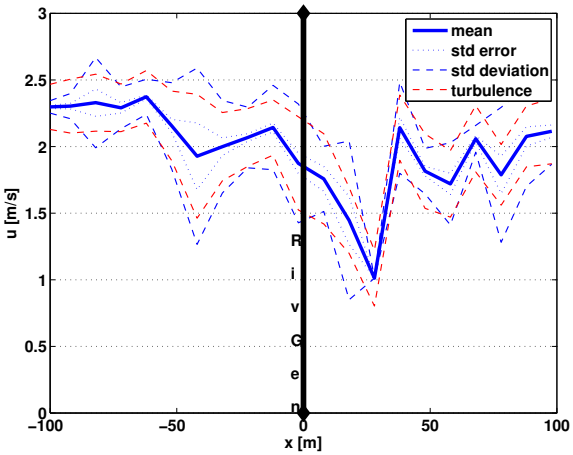

Figure 6: Streamwise flow u upstream and downstream of the turbine ($-6 < y < 8$ m). Results are the average from 563 stations lasting at least 10 minutes each. The blue dotted line is the standard error in determining the mean flow at each y. The blue dashed line is the standard deviation of individual stations. The red dashed line is variation expected from the measured turbulence intensity. The turbine location is shown by the black line ($x = 0$ m).

3.3 Streamwise variations (inflow and wake)

The alongstream pattern of the streamwise mean flow shown in Figure 6 is dominated by the presence of the RivGen turbine and the reduction in flow immediately downstream of the turbine ($0 < x < 20$ m). The reduction in the mean flow is significant, from 2 m/s to 1 m/s, and is consistent with momentum deficit expected from energy extraction. Curiously, an increase in turbulence intensity, as expected for wake-added turbulence, is not observed. The wake results are poorly constrained, because only a few stations were collected in this region (see Figure 3), and thus should be interpreted with some skepticism. Furthermore, these results are confounded by the strong lateral shears across the turbine (i.e., Figure 4), such that any non-uniformity in sampling with bias particular x slices. For example, the upstream measurement have shown a reduction in flow and in increase in the variability around $x = -50$ m, which is coincident with a gap in the stations (see Figure 3) and biased sampling towards the negative y.

Despite the caveats in the streamwise pattern, it is worth nothing that the velocity deficit recovers around $x = 30$ m, which is 20 turbine diameters downstream.

3.4 Turbulence spectra and coherence

The temporal variability in the velocity components for a given location is shown in Figure 7 as the turbulent kinetic energy (TKE) spectra upstream ($x \approx -75$ m) and downstream ($x \approx 50$ m) of the turbine. Spectral are calculated using 10-minutes of motion-corrected velocity data from a Nortek Vector mounted on a 'turbulence torpedo' (see Figure 2) hanging from a davit at turbine hub height ($z = -2$ m). Motion-compensated spectra have been demonstrated by *Thomson et al.* (2013); *Kilcher et al.* (2014), and the methods herein are the same. The corrections are minor, because the 'turbulence torpedo' is fared and does not introduce much motion. Spectral are similar up and downstream of the turbine, other than some elevation in the v component at mid-frequencies.

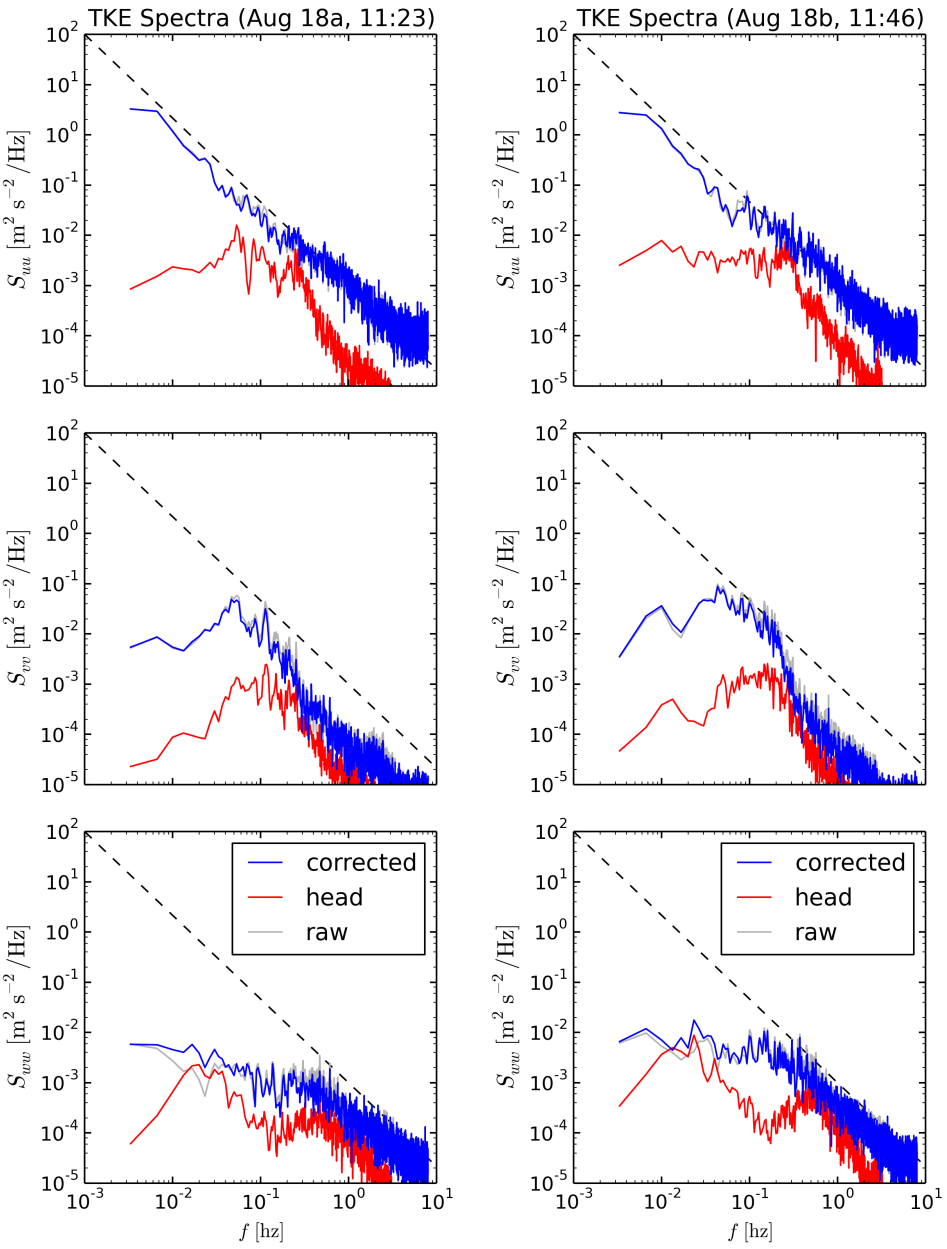

Figure 7: Turbulent kinetic energy spectra density versus frequency for the different velocity components (top is u, middle is v, bottom is w) measured upstream (left) and downstream (right) of the turbine. Corrected spectra (blue lines) use the motion of the instrument head (red) to remove motion from the raw spectra (grey lines). Spectral are calculated using 10-minutes of motion-corrected velocity data from a Nortek Vector mounted on a 'turbulence torpedo' hanging from a davit at turbine hub height ($z = -2$ m).

This is most likely because the downstream measurement was beyond the region of significant wake (see Figure 6).

The spectra of all components show an expected $f^{-5/3}$ power law at high frequencies, consistent with the isotropic cascade of energy from large scales to small scales through the inertial range. At lower frequencies, the u components continue the power law, but the v and w components have maxima at $f \approx 0.06$ Hz and $f \approx 0.2$ Hz, respectively. Assuming that the eddies are 'frozen' as they advect with the mean flow (i.e., Taylor's hypothesis), time and length scales are related as

$$2\pi l = \frac{\bar{u}}{f}, \tag{4}$$

where f is the cyclic frequency in a TKE spectrum. Thus, the length scales of the maxima in v and w are $l_v \approx 6$ m and $l_w \approx 2$ m. These length scales are consistent with the expectation that the 6 to 7 m depth of the main river channel limits the scale of 3D isotropic turbulence and that vertical motions w' are further limited by the distance from the measurement volume to the nearest boundary (here, the surface, which is 2 m away).

More puzzling is the lack of a maxima in the u component spectra, which would be expected to be similar to the v component. This may be related to leakage at low frequencies, where subtle changes in station keeping of the boat against the river flow may add additional variance. Alternatively, the low frequency energy in the u component could be contaminated by deviations from the frozen field approximation, which are expected for the large scales that take a relatively long time (> 10 s) to advect past the instrument. Although the physical reason and relation to $f^{-5/3}$ is unclear, the empirical result is useful: the temporal variations in the flow are dominated by large fluctuations over long time scales (> 10 s).

The turbulence spectrum is equivalent to the lagged auto-correlation of a given velocity time series. Figure 8 shows this calculation for a doppcat measurement upstream of the turbine, as well as the lagged correlation *between* two simultaneous doppcat measurements separated by 10 m in x. Consistent with the upstream TKE spectrum, the auto-correlation result shows significant correlations on time lags of up to ± 40 s. The correlation between two simultaneous independent measurements shows almost an identical result. This is contrary to the expectation of a distinct, sign-definite lag between the two measurements, as would be expected if the flow was truly a frozen signal advecting along or was wave-like. Such a flow would be the ideal case for implementing feed-forward control in a turbine, because an upstream measurement could be projected to the turbine with a known time lag.

Despite the general lack of coherent lags in simultaneous flow measurements at various separation distances (other examples are similar to Figure 8), the inflow at the site RivGen is still amenable to control strategies. The streamwise flow appears to be coherent at large space and time scales. On short space and time scales (i.e., small eddies), the turbulence likely evolves too quickly to observe lags, and on longer time scales the lags are essentially zero for separations of O(10 m). The zero lag result dominates because the longer scales contain the most energy. Thus, at any individual fixed point, such as the turbine location, the most robust preview of the flow would be the previous 10 to 30 s of flow *at that location*. An upstream measurement would have no increased skill relative to this self-forecast, because the only thing different at the upstream measurement location would be the small, incoherent eddies. Restated: the large velocity fluctuations tend to last at least 10 s, and on those time scales localized measurements are equivalent to any upstream measurement. (This is akin to the famous 'dummy' forecast in meteorology: synoptic weather

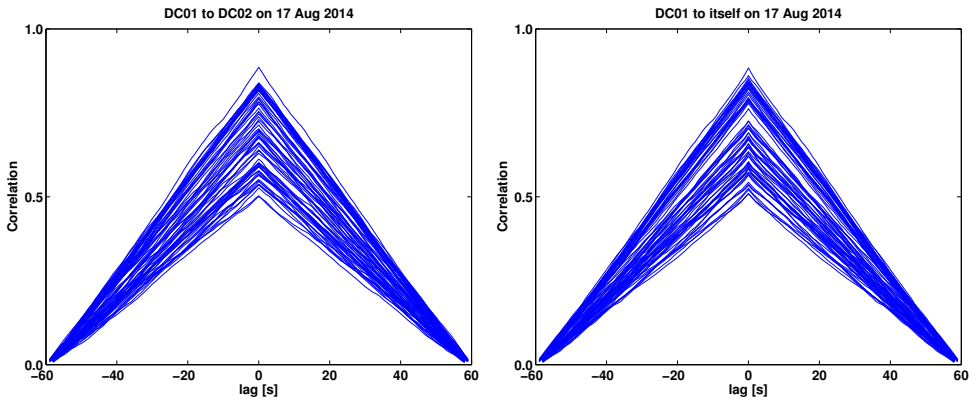

Figure 8: Lagged correlations between two upstream doppcat velocity measurements separated by 10 m (left) and the same calculation for single doppcat measurement (right). Correlations are calculated using raw velocity data (1 Hz) in one-minute ensembles, after correction for platform motion using the GPS data.

patterns last longer than one day, and thus a simple forecast that tomorrow's weather will be like today's weather is quite skillful.)

4 Conclusions

At this site, and likely at many other river sites, flow is generally steady at a given location, but flow varies dramatically between locations, particularly across the river. The primary result here is that 1) a lateral change in position of a few meters results in changes to flow speed that far exceed the turbulence fluctuations at any given location and 2) the turbulence is dominated by long time scales. Simply put, this is a site for which it is more important to know where you are than to know what time it is.

5 Acknowledgements

Joe Talbert, Alex deKlerk, and Curtis Rusch provided excellent technical support in the field. Funded by the US Dept of Energy.

References

Kilcher, L., J. Thomsoon, and J. Colby, Determing the spatial coherence of turbulence at MHK sites, in *Proceedings of the 2nd Marine Energy Technical Symposium (METS)*, edited by ', 2014.

Thomson, J., B. Polagye, V. Durgesh, and M. Richmond, Measurements of turbulence at two tidal energy sites in Puget Sound, WA, *J. Ocean. Eng.*, *37*(3), 363–374, 2012.

Thomson, J., et al., Tidal turbulence spectra from a compliant mooring, in *Proceedings of the 1st Marine Energy Technical Symposium (METS)*, 2013.